

# blood

2010 116: 653-660  
Prepublished online Mar 25, 2010;  
doi:10.1182/blood-2009-12-256644

## Hedgehog regulates distinct vascular patterning events through VEGF-dependent and -independent mechanisms

Leigh Coultas, Erica Nieuwenhuis, Gregory A. Anderson, Jorge Cabezas, Andras Nagy, R. Mark Henkelman, Chi-Chung Hui and Janet Rossant

---

Updated information and services can be found at:

<http://bloodjournal.hematologylibrary.org/cgi/content/full/116/4/653>

Articles on similar topics may be found in the following *Blood* collections:

[Vascular Biology](#) (167 articles)

---

Information about reproducing this article in parts or in its entirety may be found online at:

[http://bloodjournal.hematologylibrary.org/misc/rights.dtl#repub\\_requests](http://bloodjournal.hematologylibrary.org/misc/rights.dtl#repub_requests)

Information about ordering reprints may be found online at:

<http://bloodjournal.hematologylibrary.org/misc/rights.dtl#reprints>

Information about subscriptions and ASH membership may be found online at:

<http://bloodjournal.hematologylibrary.org/subscriptions/index.dtl>

Blood (print ISSN 0006-4971, online ISSN 1528-0020), is published semimonthly by the American Society of Hematology, 1900 M St, NW, Suite 200, Washington DC 20036.

Copyright 2007 by The American Society of Hematology; all rights reserved.



## Hedgehog regulates distinct vascular patterning events through VEGF-dependent and -independent mechanisms

Leigh Coultas,<sup>1</sup> Erica Nieuwenhuis,<sup>1</sup> Gregory A. Anderson,<sup>2,3</sup> Jorge Cabezas,<sup>4</sup> Andras Nagy,<sup>5,6</sup> R. Mark Henkelman,<sup>2,3</sup> Chi-Chung Hui,<sup>1,6</sup> and Janet Rossant<sup>1,6</sup>

<sup>1</sup>Hospital for Sick Children Research Institute, Developmental and Stem Cell Biology Program, Toronto; <sup>2</sup>Mouse Imaging Centre (MICe), Hospital for Sick Children, Toronto Centre for Phenogenomics, Toronto; <sup>3</sup>Department of Medical Biophysics, University of Toronto, Toronto; <sup>4</sup>Toronto Centre for Phenogenomics, Toronto; <sup>5</sup>Samuel Lunenfeld Research Institute, Mount Sinai Hospital, Toronto; and <sup>6</sup>Department of Molecular Genetics, University of Toronto, Toronto, ON

**Despite the clear importance of Hedgehog (Hh) signaling in blood vascular development as shown by genetic analysis, its mechanism of action is still uncertain. To better understand the role of Hh in vascular development, we further characterized its roles in vascular development in mouse embryos and examined its interaction with vascular endothelial growth factor (VEGF), a well-known signaling pathway essential to blood vascular devel-**

**opment. We found that VEGF expression in the mouse embryo depended on Hh signaling, and by using genetic rescue approaches, we demonstrated that the role of Hh both in endothelial tube formation and Notch-dependent arterial identity was solely dependent on its regulation of VEGF. In contrast, overactivation of the Hh pathway through deletion of Patched1 (Ptch1), a negative regulator of Hh signaling, resulted in reduced vascu-**

**lar density and increased Delta-like ligand 4 expression. The Ptch1 phenotype was independent of VEGF pathway dysregulation and was not rescued when Delta-like ligand 4 levels were restored to normal. These findings establish that Hh uses both VEGF- and Notch-dependent and -independent mechanisms to pattern specific events in early blood vascular development. (*Blood*. 2010;116(4):653-660)**

### Introduction

The blood vascular system is the first organ to develop in the mammalian embryo, establishing a basic circulatory system between embryonic (E) day 7.5 and E8.5. The vessels that initially comprise the blood vascular system form by the process of vasculogenesis: the assembly of endothelial precursors (angioblasts) into simple endothelial tubes in the absence of preexisting vessels. Failure to establish these initial vessels results in growth arrest and embryonic lethality by E9.5.<sup>1</sup> Subsequent remodeling and expansion of these and other vessels requires the intricate and coordinated process of angiogenesis: the branching, splitting, pruning, and proliferation of preexisting vessels. The Hedgehog (Hh) signaling pathway is known to play an important role in blood vessel development,<sup>2</sup> but its mechanism of action remains incompletely defined. To better understand this role, we have used the mouse embryo as a model to examine the interplay between Hh and vascular endothelial growth factor (VEGF) signaling, another pathway essential for blood vascular development.<sup>3</sup>

The interplay between Hh and VEGF in vascular development is exemplified in the establishment of artery/vein identity in zebrafish. In this pathway, notochordal Hh induces expression of VEGF in neighboring somites, which in turn induces Notch-dependent arterial identity in endothelial cells.<sup>4</sup> In mice, Notch signaling is essential for artery specification,<sup>5</sup> and numerous receptors and ligands for this pathway become restricted to arteries,<sup>6</sup> key among them are Notch1,<sup>7</sup> Notch4,<sup>8</sup> and Delta-like ligand 4 (Dll4).<sup>9</sup> Although the role for Notch in assignment of arterial identity in mice is unequivocal, the requirement for either

Hh or VEGF upstream of Notch in vivo during mouse development has not been determined.

Hh is also essential for endothelial tube formation. In mouse embryos, this requirement is limited to the anterior (but not posterior) region of the dorsal aorta and to the vessels of the yolk sac.<sup>10</sup> Endothelial cells express the Hh-binding receptor Patched1 (Ptch1),<sup>10,11</sup> and Hh ligand can induce endothelial cord and tube formation in vitro.<sup>10,12</sup> However, mice lacking the common Hh signal transducer smoothed (Smo), specifically in endothelial cells, develop normally into adulthood,<sup>13</sup> arguing the role of Hh in endothelial tube formation is nonautonomous. Hh is known to induce expression of proangiogenic cytokines, including VEGF in nonendothelial tissues,<sup>11</sup> and mice lacking VEGF experience severe defects in blood vessel development, resulting in embryonic lethality around the same time as embryos lacking Smo,<sup>14,15</sup> making it a likely candidate for a downstream mediator of Hh in endothelial tube formation.

In this study, we investigated the interaction between Hh and VEGF signaling pathways in vasculogenesis in the mouse embryo. We found that Hh is required for VEGF expression during mouse vasculogenesis and that both were required for artery/vein identity in addition to their role in endothelial tube formation. Restoration of VEGF pathway activation to endothelial cells of Hh mutants was sufficient to rescue both the arterial identity and endothelial tube formation and defects in Hh mutants. In contrast, we found that hyperactivation of the Hh signaling pathway through deletion of Ptch1 caused increased aorta diameter and increased expression of

Submitted November 29, 2009; accepted March 11, 2010. Prepublished as *Blood* First Edition paper, March 25, 2010; DOI 10.1182/blood-2009-12-256644.

The publication costs of this article were defrayed in part by page charge payment. Therefore, and solely to indicate this fact, this article is hereby marked "advertisement" in accordance with 18 USC section 1734.

The online version of this article contains a data supplement.

© 2010 by The American Society of Hematology

the arterial Notch ligand *Dll4*; however, levels of VEGF and its major receptors were not affected in *Ptch1* mutants. Together, these results demonstrate that Hh signaling modulates distinct vascular patterning events in mammalian embryos through both VEGF-dependent and -independent mechanisms.

## Methods

### Mice

Experiments were approved by the Animal Care Committee of the Hospital for Sick Children and were conducted in accord with guidelines established by the Canadian Council on Animal Care. The following mouse lines were used in this study: *Smo* (generated by crossing *Smo<sup>fllox/fllox16</sup>* with a ubiquitous cre deleter strain, resulting in *Smo<sup>del/+</sup>* followed by outcrossing to wild-type CD1 strain mice to remove cre) and *Ptch1* (generated by crossing *Ptch1<sup>fllox/fllox17</sup>* with a ubiquitous cre deleter strain, resulting in *Ptch1<sup>del/+</sup>* followed by outcrossing to wild-type CD1 strain mice to remove cre). *Flt1<sup>lacZ/+</sup>*,<sup>18</sup> *Dll4<sup>lacZ/+</sup>*,<sup>9</sup> and *VEGF<sup>hyppo/+14</sup>* were all maintained on a CD1 background. Embryos from timed pregnancy were collected either at E8.5 (6- to 8-somite stage), or at E9.5 (approximately 20-somite stage). Noon on the day the plug was observed was considered to be E0.5.

### Whole-mount in situ hybridization

Whole-mount in situ hybridization was performed by the use of a modified version of Lickert et al<sup>19</sup> but with the following modifications: proteinase K treatment was replaced with a 20-minute treatment with 3% hydrogen peroxide, levamisole was excluded from all solutions, and (with the exception of VEGF assessment in *Smo* mutant and control embryos), methanol fixation was replaced with a 20-minute treatment with 50mM sodium azide before hydrogen peroxide treatment. Antisense DIG-labeled RNA probes were transcribed from sequence verified clones encoding mouse *Dll4* (a generous gift from Prof Antonio Duarte, Instituto Gulbenkian de Ciéncia, Oeiras, Portugal) or mouse VEGF. Stained embryos were imaged with a Leica MZ16F stereoscope equipped with a Micropublisher 5.0 RTV (QImaging) camera and Volocity software (Improvision). All postacquisition image analysis and modification were conducted with Photoshop (Adobe).

### Whole-mount immunofluorescence and optical projection tomography imaging

Whole-mount immunohistochemistry was performed by the use of a modified version of Walls et al.<sup>20</sup> but methanol fixation was replaced with a 20-minute treatment with 50mM sodium azide in phosphate-buffered saline containing 0.1% Tween 20. Stained embryos were cleared in a graded series of glycerol in phosphate-buffered saline (up to 80%) before imaging. Epifluorescence imaging was performed by the use of a Zeiss Axiovert 200M inverted microscope with a Ph1 Plan-Neofluar 5×/0.15 NA objective. Images were captured with an AxioCam HRm camera (Zeiss) with Axiovision 4.6 software (Zeiss). All postacquisition image analysis and modification were conducted by the use of Photoshop (Adobe). Confocal imaging was performed with a Zeiss LSM510 META confocal microscope, Plan-Neofluar 25×/0.8 NA immersion correction objective with pinhole set to 1 Airy Unit. YZ and XZ stacks were compiled from the original data with Volocity software (Improvision). Optical projection tomography (OPT) was performed as previously described.<sup>20</sup>

### Quantitative reverse transcription polymerase chain reaction

In all cases, the extraembryonic structures of yolk sac, allantois, and amnion were removed from the embryo before RNA was extracted. Where indicated in Figures 1 and 2, embryos were further subdivided into specific embryonic regions. Total RNA was extracted from embryos by the use of Trizol Reagent (Invitrogen) and reverse transcribed (RT) with the QuantiTect RT kit (QIAGEN) according to the manufacturer's instructions. Quantitation of gene expression was performed by real-time polymerase chain reaction (PCR) with a LightCycler 480 (Roche). Each reaction was performed in technical triplicate with 2X SYBR mix (Roche) containing

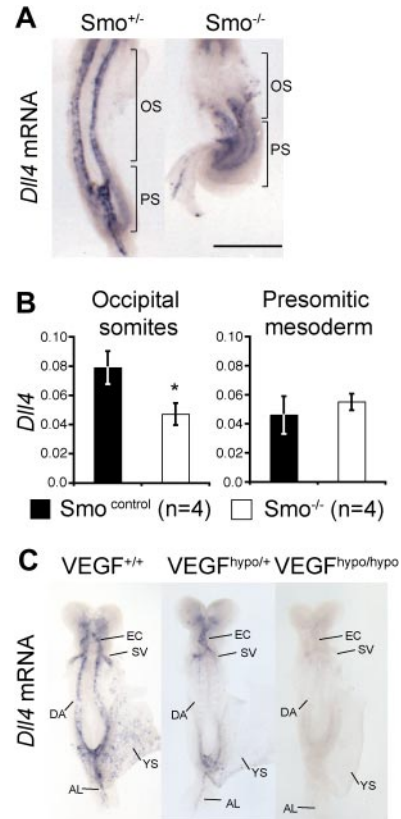


**Figure 1. Hh and VEGF are required for arterial identity in mice.** (A) Whole-mount in situ hybridization for *Dll4* mRNA in E8.5 (approximately 8-somite stage) *Smo<sup>+/+</sup>* and *Smo<sup>-/-</sup>* embryos. Brackets indicate the occipital somite (OS) and presomitic/primitive streak (PS) regions of the embryo microdissected for Q-RT-PCR in panel B. Scale bar equals 500  $\mu$ m. (B) Q-RT-PCR for *Dll4* mRNA in *Smo<sup>+/+</sup>* (*Smo<sup>+/+</sup>*, n = 2 and *Smo<sup>-/-</sup>*, n = 2) and *Smo<sup>-/-</sup>* (n = 4) littermates. Q-RT-PCR was performed on distinct regions of 8-somite stage embryos corresponding to the occipital somites region (labeled OS in panel A) and presomitic region (labeled PS in panel A) in control or mutant embryos. Data are presented as *Dll4* expression relative to the loading control, *Polr2a*. Asterisk indicates statistical significance between control and mutant sample groups,  $P < .05$ . (C) Whole-mount in situ hybridization for *Dll4* mRNA in E8.5 (7- to 8-somite stage) *VEGF<sup>+/+</sup>*, *VEGF<sup>hyppo/+</sup>*, and *VEGF<sup>hyppo/hypo</sup>* embryos. Representative embryos from *VEGF<sup>+/+</sup>* (n = 4), *VEGF<sup>hyppo/+</sup>* (n = 3), and *VEGF<sup>hyppo/hypo</sup>* (n = 2) littermates are shown. EC indicates endocardium; SV, sinus venosus; DA, dorsal aorta; YS, yolk sac plexus; and AL, allantoic artery.

100 ng of cDNA and 300 nmol/L each of gene-specific forward and reverse oligonucleotides (ie, *Vegf* sense caggctgctgaacgatgaa, antisense tatgtgctgctgttgtag; *Flt1* sense caagcaggccagactctctt, antisense gggagtgatgctcagcctt; *Dll4* sense tgccctgggaagtatctctac, antisense tagagtcctctggagagcaaa; *Ptch1* sense gcgctaattgtctgaccaca, antisense agcacaatgttccaactcc; *Gli1* sense ctcaagggccaatcatgc antisense taggacttccagacagcctc; *Fli1/Kdr* sense ttggcaaatacaaccctcaga, antisense gcagaagatactgtcaccaccg; *Nrp1* sense aaccacatttcgatttggga, antisense aaggtgcaatctctcccacag; and *Polr2a* sense cccaaactgggggactaat, antisense aggaagcccatgaaacac) in a 50-cycle reaction (95°C 10 seconds, 60°C 10 seconds, 72°C 10 seconds). Specificity of oligonucleotides was confirmed by melt curve analysis and gene expression determined by relative quantification with correction for amplification efficiency for each oligonucleotide pair (determined by standard curve analysis). All data were analyzed by the  $\Delta$ CT method and expressed as gene expression relative to the internal loading control, *Polr2a*.

## Results

### Hh and VEGF are required upstream of Notch for arterial identity in mice

Because the Notch ligand *Dll4* is specific to arterial endothelial cells and is essential for arterial identity in mouse,<sup>9</sup> we chose to

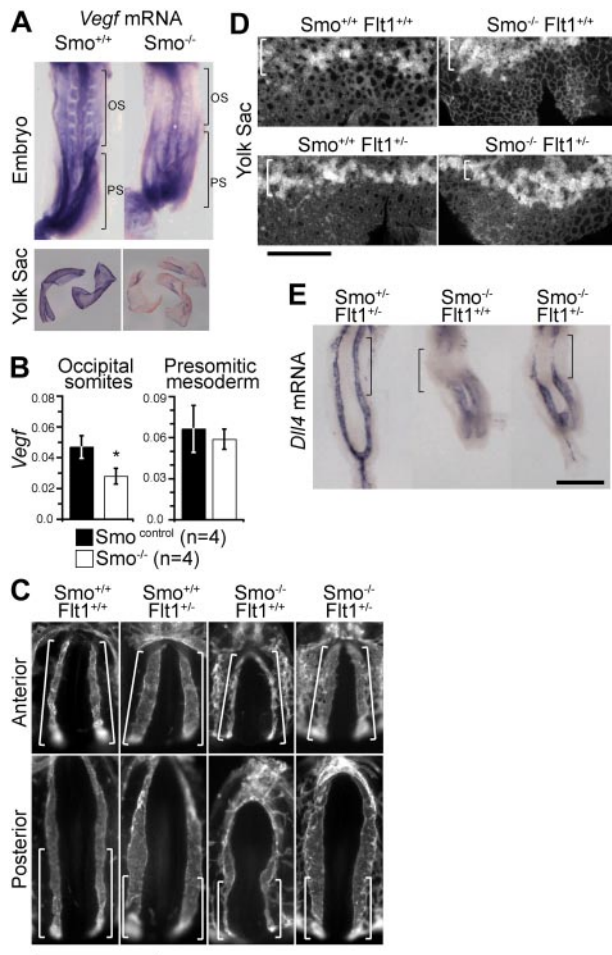


**Figure 2. Hh requires VEGF for arterial identity and endothelial tube formation.** (A) Whole-mount in situ hybridization for *Vegf* mRNA in E8.5 *Smo* mutant embryos. Representative embryos and all yolk sacs from 8 somite stage *Smo*<sup>+/+</sup> (n = 2) and *Smo*<sup>-/-</sup> (n = 3) littermates are shown. Brackets indicate the occipital somite (OS) and presomitic/primitive streak (PS) regions of the embryo microdissected for Q-RT-PCR in panel B. (B) Q-RT-PCR for *Vegf* mRNA in *Smo* control (*Smo*<sup>+/+</sup>, n = 2 and *Smo*<sup>+/-</sup>, n = 2) and *Smo*<sup>-/-</sup> (n = 4) embryos. Q-RT-PCR was performed on distinct regions of 8-somite stage littermates corresponding to the occipital somites region (labeled OS in panel A) and presomitic region (labeled PS in panel A) in control or mutant embryos. Data are presented as *Vegf* expression relative to the loading control, *Polr2a*. Asterisk indicates statistical significance (*t* test) between control and mutant sample groups, *P* < .05. (C) Whole-mount PECAM1 staining of E8.5 (approximately 8-somite stage) *Smo*; *Flt1* compound mutant embryos. Representative examples of littermate *Smo*<sup>+/+</sup>; *Flt1*<sup>+/+</sup> (n = 2), *Smo*<sup>+/+</sup>; *Flt1*<sup>+/-</sup> (n = 2), *Smo*<sup>-/-</sup>; *Flt1*<sup>+/+</sup> (n = 1), and *Smo*<sup>-/-</sup>; *Flt1*<sup>+/-</sup> (n = 4) embryos are shown. Brackets indicate the region of the dorsal aorta affected in *Smo*<sup>-/-</sup>; *Flt1*<sup>+/+</sup> embryos and located in *Smo*<sup>-/-</sup>; *Flt1*<sup>+/-</sup> embryos. The affected region corresponds exactly to the location of the somites in each embryo. Scale bar represent 500  $\mu$ m. (D) Whole-mount PECAM1 staining of E8.5 (approximately 8-somite stage) *Smo*; *Flt1* compound mutant yolk sacs. Representative examples of littermate *Smo*<sup>+/+</sup>; *Flt1*<sup>+/+</sup> (n = 2), *Smo*<sup>+/+</sup>; *Flt1*<sup>+/-</sup> (n = 2), *Smo*<sup>-/-</sup>; *Flt1*<sup>+/+</sup> (n = 1), *Smo*<sup>-/-</sup>; *Flt1*<sup>+/-</sup> (n = 4) embryos are shown. Brackets indicate the position of the blood islands. Scale bar represents 500  $\mu$ m. (E) Whole-mount in situ hybridization for *Dll4* mRNA in E8.5 (approximately 8-somite stage) *Smo*<sup>+/+</sup>; *Flt1*<sup>+/-</sup> (n = 1), *Smo*<sup>-/-</sup>; *Flt1*<sup>+/+</sup> (n = 3), and *Smo*<sup>-/-</sup>; *Flt1*<sup>+/-</sup> (n = 2) littermate embryos. Bracket indicates occipital somite region. Scale bar represents 500  $\mu$ m.

investigate its expression as a readout for arterial fate in mice in which Hh signaling was blocked (*Smo*<sup>-/-</sup>). *Dll4* mRNA expression was readily detected in the dorsal aorta of 8 somite (E8.5) *Smo*<sup>+/-</sup> embryos (Figure 1A). In contrast, *Dll4* mRNA was extremely weak or absent from the anterior portion of the aorta underlying the occipital somites of *Smo*<sup>-/-</sup> embryos but normal in the portion underlying the presomitic tail bud region (Figure 1A). By using quantitative RT-PCR (Q-RT-PCR), we confirmed that *Dll4* mRNA

was significantly reduced in the occipital somite region but expressed at normal levels in the presomitic region of *Smo*<sup>-/-</sup> embryos (Figure 1B).

We next examined *Dll4* expression in mice carrying a hypomorphic allele for VEGF. Embryos homozygous for this allele phenotype VEGF heterozygote-null embryos.<sup>14</sup> *Dll4* mRNA was lost from all arterial endothelial populations in VEGF<sup>hypos/hypo</sup> embryos (Figure 1C). Interestingly, we observed a dose-dependent reduction of *Dll4* mRNA levels in VEGF<sup>hypos/+</sup> and VEGF<sup>hypos/hypo</sup> embryos compared with littermate controls (Figure 1C). This result is consistent with observations made during angiogenesis that suggest arterial identity is defined by a gradient of VEGF activity.<sup>21,22</sup> These results demonstrate that both Hh and VEGF are required upstream of Notch for arterial identity in mammalian embryos, but that although the role of Hh is region specific, VEGF is required for all arterial populations.

### Hh and VEGF are required for tube formation in mouse embryos

Embryos lacking Hh signaling experience region-specific defects in endothelial tube formation.<sup>10</sup> Because VEGF mutants also have severe defects in vessel formation,<sup>14,15,23</sup> we sought to determine the similarity between the Hh and VEGF phenotypes. Consistent with previous reports,<sup>10</sup> we found tube formation defects in the anterior dorsal aorta and yolk sac vessels of 8-somite stage (E8.5) *Smo*<sup>-/-</sup> embryos but not in the posterior dorsal aorta when staining with the pan-endothelial marker platelet/endothelial cell adhesion molecule-1 (PECAM1; supplemental Figure 1A, available on the *Blood* Web site; see the Supplemental Materials link at the top of the online article). Whole-mount PECAM1 staining revealed the dorsal aortas of 8-somite stage VEGF<sup>hypos/hypo</sup> embryos to be severely constricted compared with their control littermates (supplemental Figure 1B). Tube formation was affected along the entire length of the VEGF<sup>hypos/hypo</sup> aorta, demonstrating that VEGF is required for tube formation in all endothelial cells of the aorta. Yolk sac vessels were essentially absent from VEGF<sup>hypos/hypo</sup> embryos, preventing assessment of tube formation in this population.

In addition to reduced vessel diameter, whole-mount PECAM1 staining revealed an additional vascular patterning defect in *Smo* mutants. Whereas the region of the embryo underlying the lateral plate mesoderm of control embryos was avascular, in *Smo* mutants, this region was occupied by a vascular plexus, which appeared to connect the dorsal aorta to the yolk sac vascular plexus (arrowheads in supplemental Figure 1A). This phenotype was not evident in VEGF<sup>hypos/hypo</sup> embryos (arrowheads in supplemental Figure 1B), suggesting the requirement for Hh in this process is independent of VEGF.

### Hh is required for VEGF expression in a regionally restricted fashion in mouse embryos

Given that VEGF loss-of-function mutants experienced similar arterial identity and tube formation defects as *Smo* mutants, we next sought to assess whether VEGF expression was reduced in *Smo* mutants. Whole-mount in situ hybridization for *Vegf* mRNA was used to assess *Vegf* levels in *Smo*<sup>-/-</sup> and littermate controls. *Vegf* mRNA levels in 6- and 8-somite stage *Smo*<sup>-/-</sup> embryos were reduced specifically in the occipital somites compared with their wild-type littermates but appeared normal in the presomitic mesoderm of the tail bud (Figure 2A; supplemental Figure 2). Q-RT-PCR showed *Vegf* mRNA levels to be significantly reduced in the cephalic somite region but not the tail bud of *Smo*<sup>-/-</sup> embryos compared with their littermate controls (Figure 2B). Reduced *Vegf*

mRNA also was evident in the yolk sacs of *Smo* mutants at the 6- and 8-somite stages by whole-mount in situ hybridization (Figure 2A; supplemental Figure 2). Collectively, these results indicate that in mouse embryos, Hh is necessary for normal VEGF expression in those regions of the *Smo*<sup>-/-</sup> embryo where Hh is required for tube formation and arterial endothelial identity.

### VEGF is sufficient for endothelial tube formation and arterial identity in the absence of Hh signaling

We next sought to address whether the vascular patterning defect of *Smo*<sup>-/-</sup> embryos could be rescued by restoration of VEGF signaling. We excluded using VEGF<sup>hyper</sup> mice (which have elevated VEGF expression from the endogenous *Vegf* locus as the result of increased mRNA stability<sup>24</sup>) for this analysis because their elevated levels of VEGF require the endogenous *Vegf* promoter and hence likely require an intact Hh signaling pathway. Furthermore, VEGF expression levels vary significantly between tissues and developmental stages in the VEGF<sup>hyper</sup> embryos, and VEGF levels at the stage in which we were interested (E8.5) had not been assessed.<sup>24</sup> Therefore, we could not be certain this mutant would generate sufficient levels of VEGF to test the epistatic relationship between VEGF and *Smo*. Instead, because *Smo* mutants retained some residual levels of VEGF expression (~60% of normal) in areas of defective vascular development, we reasoned that increasing the sensitivity of endothelial cells to the VEGF still present might rescue the *Smo* phenotype. We addressed this by breeding *Smo* mutants to mice lacking the high-affinity VEGF receptor *Flt1*. During vasculogenesis, *Flt1* is inhibitory for VEGF signaling and is generated both as membrane-bound and soluble isoforms.<sup>25,26</sup>

Consistent with previous observations, *Flt1*<sup>-/-</sup> embryos lacked a defined cranial plexus at E8.5 (approximately 8 somites) and developed what appeared to be severe endothelial and blood island overgrowth in the yolk sac (supplemental Figure 3A).<sup>18</sup> *Flt1*<sup>+/-</sup> embryos also showed subtle abnormalities in yolk sac and dorsal aorta vascular development, with wider vessel channels, suggesting VEGF perception is heightened in the absence of one copy of *Flt1* (Figure 2C). When we used Q-RT-PCR, we determined *Dll4* mRNA expression to be 2.1-fold greater in *Flt1* mutant embryos at E8.5 (8 somites) compared with stage-matched littermates (supplemental Figure 3B), which is consistent with VEGF-promoting arterial identity.

Because *Flt1*<sup>+/-</sup> mice presented a phenotype consistent with elevated VEGF signaling, we assessed whether removal of one copy of *Flt1* could rescue the *Smo* phenotype. Vascular morphology was assessed in *Smo*<sup>-/-</sup>;*Flt1*<sup>+/-</sup> embryos by whole-mount PECAM1 staining of embryos at E8.5. *Smo*<sup>-/-</sup>;*Flt1*<sup>+/-</sup> embryos displayed the expected constriction of the anterior dorsal aorta and yolk sac vessels at E8.5 (Figure 2C). In contrast, the dorsal aorta of *Smo*<sup>-/-</sup>;*Flt1*<sup>+/-</sup> embryos at E8.5 were of comparable diameter to those of their wild-type littermates (4 of 4 embryos; Figure 2C). In contrast, the ectopic vessels present adjacent to the dorsal aorta in the *Smo*<sup>-/-</sup> embryos were not rescued by removal of one copy of *Flt1* (Figure 2C). In the yolk sac, the majority (3 of 4) of *Smo*<sup>-/-</sup>;*Flt1*<sup>+/-</sup> embryos showed restoration of vessel diameter (Figure 2D).

In situ hybridization for *Dll4* mRNA showed only partial restoration of *Dll4* expression to the anterior dorsal aorta in *Smo*<sup>-/-</sup>;*Flt1*<sup>+/-</sup> embryos (Figure 2E). Because VEGF regulates *Dll4* expression in a dose-dependent fashion (see "Hh and VEGF are required upstream of Notch for arterial identity in mice") the removal of 1 copy of *Flt1* may not have restored VEGF signaling to high enough levels to promote complete arterialization of the

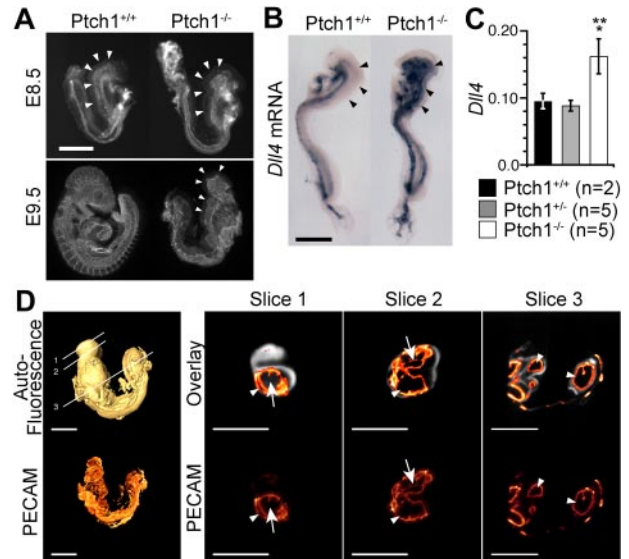


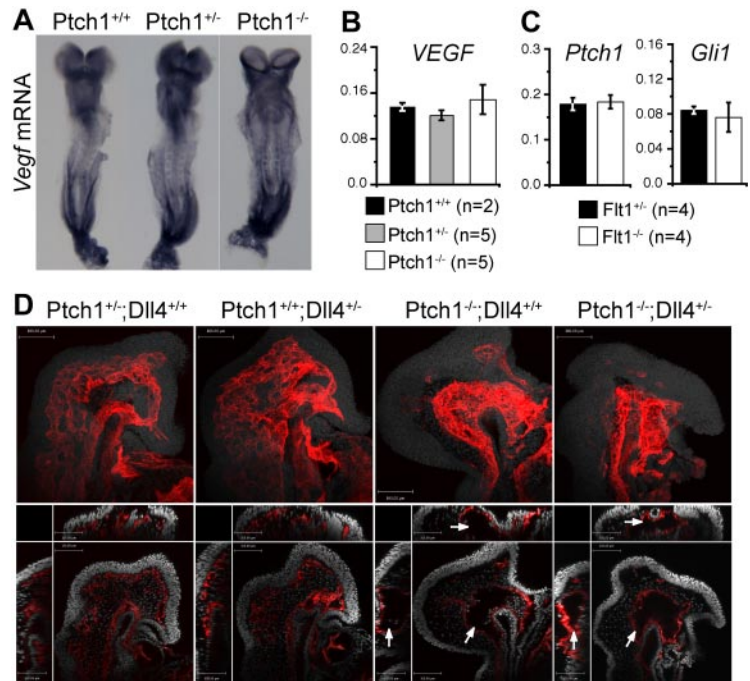
**Figure 3. Defective vascular patterning in *Ptch1* mutant embryos.** (A) Lateral view of whole-mount PECAM1 staining of E8.5 (8-somite stage) and E9.5 *Ptch1* mutant and littermate control embryos. Representative images from 8-somite stage *Ptch1*<sup>+/+</sup> (n = 3) and *Ptch1*<sup>-/-</sup> (n = 3) embryos are shown. Arrowheads indicate cranial plexus region. Scale bar represents 500  $\mu$ m. (B) Whole-mount in situ hybridization for *Dll4* mRNA in E8.5 (8-somite stage) *Ptch1* mutant embryos. Representative embryos from *Ptch1*<sup>+/+</sup> (n = 2) and *Ptch1*<sup>-/-</sup> (n = 2) littermate embryos are shown. Arrowheads indicate the region in which *Dll4* is ectopically expressed in *Ptch1* mutants versus controls. Scale bar represents 500  $\mu$ m. (C) Q-RT-PCR for *Dll4* mRNA in *Ptch1*<sup>+/+</sup> (n = 2), *Ptch1*<sup>+/-</sup> (n = 5), and *Ptch1*<sup>-/-</sup> (n = 5) embryos. Q-RT-PCR was performed on 8-somite stage embryos from which the yolk sac, allantois, and amnion had been removed. Data are presented as *Dll4* expression relative to the loading control, *Polr2a*. Single asterisk indicates statistical significance (*t* test) between *Ptch1*<sup>+/+</sup> and *Ptch1*<sup>-/-</sup> sample groups (*P* < .05). Double asterisk indicates statistical significance (*t* test) between *Ptch1*<sup>+/-</sup> and *Ptch1*<sup>-/-</sup> sample groups, (*P* < .005). (D) FDR-OPT images of an E9.5 *Ptch1*<sup>-/-</sup> embryo. Top left side is a surface-rendered image of the 3D reconstructed autofluorescence signal with locations of digital slices shown in right side panels indicated. Bottom left side is a 3D reconstruction of PECAM1-Cy3 signal alone. Right side images are digital slices from 3D reconstructed FDR-OPT data, top are PECAM1-Cy3 signal overlaid on autofluorescence signal, bottom are PECAM1-Cy3 signal from the same slice alone. Arrows indicate PECAM1<sup>+</sup> structures surrounding other tissue (autofluorescence signal present), arrowheads indicate PECAM1<sup>+</sup> signal encompassing hollow space (autofluorescence signal not present).

dorsal aorta. It remains to be addressed whether removal of both copies of *Flt1* could fully restore *Dll4* expression and arterial identity in *Smo*<sup>-/-</sup> aortas. These results demonstrate that Hh does not act cell autonomously to regulate endothelial tube formation and arterial identity but instead acts to induce VEGF in nonendothelial tissues, which then regulates tube formation and arterial identity.

### Vascular patterning in *Ptch1* mutants is phenotypically similar to *Flt1* mutants

Because Hh ligand is sufficient to promote an angiogenic response when added exogenously to organ cultures or to mice and chicks,<sup>10,11,13,27</sup> we sought to determine what effect overactivation of the Hh pathway would have on early stages of vascular development and its relationship to VEGF by assessing vascular development in embryos lacking the inhibitory Hh receptor *Ptch1*. PECAM1 staining revealed that the normally branched network of small-caliber capillaries that comprised the cephalic plexus of E8.5 (8 somite) *Ptch1*<sup>+/+</sup> embryos was absent in stage matched *Ptch1*<sup>-/-</sup> littermates (Figure 3A,D). Instead, these embryos presented a dilated dorsal aorta with few side branches and no anterior cardinal vein, similar to *Flt1* mutants. Whole-mount in situ hybridization at

**Figure 4. *Ptch1* vascular phenotype is independent of VEGF and Notch.** (A) Whole-mount in situ hybridization for *Vegf* mRNA in E8.5 *Ptch1* mutants. Representative embryos from 8-somite stage *Ptch1*<sup>+/+</sup> (n = 4), *Ptch1*<sup>+/-</sup> (n = 5), and *Ptch1*<sup>-/-</sup> (n = 3) littermate embryos are shown. (B) Q-RT-PCR for *Vegf* mRNA in *Ptch1*<sup>+/+</sup> (n = 2), *Ptch1*<sup>+/-</sup> (n = 5), and *Ptch1*<sup>-/-</sup> (n = 5) embryos. Q-RT-PCR was performed on 8-somite stage littermates from which the yolk sac, allantois, and amnion had been removed. Data are presented as gene expression relative to the loading control, *Polr2a*. (C) Q-RT-PCR for *Ptch1* and *Gli1* mRNA in *Flt1*<sup>+/+</sup> (n = 4) and *Flt1*<sup>-/-</sup> (n = 4) embryos. Q-RT-PCR was performed on 7- to 8-somite stage littermates from which the yolk sac, allantois, and amnion had been removed. Data are presented as gene expression relative to the loading control, *Polr2a*. (D) Confocal images for whole-mount PECAM1-stained *Ptch1*; *Dll4* compound mutants. Representative embryos from 8-somite stage *Ptch1*<sup>+/+</sup>; *Dll4*<sup>+/+</sup> (n = 2), *Ptch1*<sup>+/+</sup>; *Dll4*<sup>+/-</sup> (n = 2), *Ptch1*<sup>-/-</sup>; *Dll4*<sup>+/+</sup> (n = 2), *Ptch1*<sup>-/-</sup>; *Dll4*<sup>+/-</sup> (n = 3) littermates are shown. Top panel for each embryo represents projected PECAM1 stain (red) with DRAQ5 nuclear stain (gray). Bottom panels represent single confocal section (xy plane) from each embryo with yz (left) and xz (top) stacks shown (PECAM1, red; DRAQ5 nuclear, gray). Arrows indicate the abnormal, hollow vascular structures in *Ptch1*<sup>-/-</sup>; *Dll4*<sup>+/+</sup>, and *Ptch1*<sup>-/-</sup>; *Dll4*<sup>+/-</sup> embryos. Scale bars represent 100  $\mu$ m.



the 8-somite stage showed that the cephalic vasculature in *Ptch1*<sup>-/-</sup> embryos consisted exclusively of *Dll4*-expressing endothelium (Figure 3B). Increased *Dll4* expression was confirmed by Q-RT-PCR, which found *Dll4* levels to be 1.8-fold greater in *Ptch1*<sup>-/-</sup> mutants compared with their littermates (Figure 3C), similar to *Flt1* mutants. By E9.5, all *Ptch1* mutants examined showed the expected developmental arrest and had failed to turn.<sup>17</sup>

By this stage, the cranial plexus had still failed to develop in *Ptch1* mutants, and the dorsal aorta was dilated relative to their control littermates (Figure 3A). Because of the complexity of the E9.5 *Ptch1*<sup>-/-</sup> phenotype, vascular development in *Ptch1*<sup>-/-</sup> embryos was assessed by the use of high-resolution 3-dimensional frequency distance relationship (FDR)-based OPT.<sup>20</sup> The severe developmental arrest of *Ptch1* mutants before turning (approximately 10 somites) prevented meaningful comparison with control littermates at E9.5 (Figure 3A). However, the E9.5 *Ptch1* mutant vasculature can be compared with equivalently staged 8- to 9- and 10- and 11-somite stage embryos, which have been visualized by FDR-OPT previously, the data for which are freely available for analysis online.<sup>20</sup>

Overlaying the PECAM1 signal on the autofluorescence background in digital slices generated from reconstructed 3D FDR-deconvolved OPT data of *Ptch1*<sup>-/-</sup> embryos showed that the dorsal aorta and branchial arch were hollow and dilated in *Ptch1*<sup>-/-</sup> embryos, displacing much of the surrounding mesenchyme (enclosed PECAM1<sup>+</sup> structures lacking internal autofluorescence signal, arrowheads in slices 2 and 3; Figure 3D), whereas the cranial vessels formed a sheet surrounding the cranial mesenchyme (PECAM1<sup>+</sup> structure surrounding a region of autofluorescence signal, arrows in slice 1 and 2; Figure 3D). This phenotype contrasts that of *Flt1*, in which the cranial mesenchyme is completely displaced by a dilated, hollow vascular sinus.<sup>18</sup> Occasional hollow lumens could be distinguished in the *Ptch1*<sup>-/-</sup> cranial endothelial sheet, suggesting it was composed of an endothelial bi-layer lacking the organized, branched structure that normally occurs in wild-type animals (arrowhead, slice 1, Figure 3D). This analysis demonstrates that despite strong phenotypic similarity,

*Ptch1*<sup>-/-</sup> mutants do not recapitulate all aspects of the *Flt1*<sup>-/-</sup> vascular phenotype.

#### VEGF expression in *Ptch1* mutants is normal

The striking similarity of the *Ptch1* vascular phenotype to that of *Flt1* mutants prompted us to test whether an up-regulation of VEGF expression could account for the *Ptch1* vasculogenesis phenotype. Somewhat surprisingly, we could find no evidence for elevated *Vegf* mRNA in *Ptch1* mutants at E8.5 (8 somites) either by whole-mount in situ hybridization or Q-RT-PCR (Figure 4A,B). We then tested the possibility that *Ptch1*<sup>-/-</sup> endothelial cells had heightened sensitivity to VEGF because of altered VEGF receptor expression. Levels of the major VEGF receptors *Flk1* (*Kdr*, MGI:96 683) and its coreceptor *Nrp1* and *Flt1* were not altered in *Ptch1* mutants (supplemental Figure 4). Although not statistically significant, levels of *Flk1* were if anything reduced in *Ptch1* mutants, possibly because of inhibition by elevated *Dll4* levels.<sup>28-30</sup> No difference was found in the expression of the Hh-responsive genes *Gli1* or *Ptch1* between *Flt1*<sup>-/-</sup> and control embryos, suggesting that Hh signaling was not enhanced in *Flt1* mutants (Figure 4C). Collectively, these results suggest the vascular phenotype observed in *Ptch1* mutants is not attributable to dysregulated VEGF expression or perception. We next investigated expression of *Foxc1* and *Foxc2*, direct transcriptional activators of *Dll4* whose expression in endothelial cells is not regulated by VEGF,<sup>31-34</sup> in *Ptch1* mutants. Expression of both these transcription factors was normal in *Ptch1* mutant embryos, suggesting that increased *Dll4* expression was not caused by misexpression of *Foxc1* or *Foxc2*.

#### The *Ptch1* vascular phenotype is not caused by elevated *Dll4*

We then tested whether the increased *Dll4* expression we observed in *Ptch1* mutants was responsible for the *Ptch1* vascular phenotype. Because *Ptch1* mutants displayed 1.8-fold increase in *Dll4* expression over controls (see "Vascular patterning in *Ptch1* mutants is phenotypically similar to *Flt1* mutants") and *Dll4* is haploinsufficient,<sup>9,35,36</sup> we reasoned that the removal of a single copy of *Dll4*

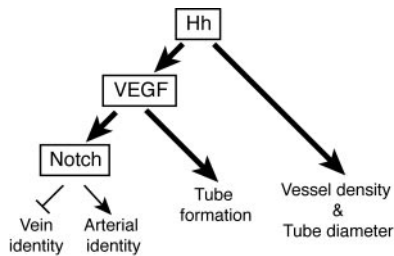


**Figure 5. Interplay between Hh, VEGF, and Notch signaling during mouse vasculogenesis.** Summary diagram illustrating the interaction between Hh and VEGF signaling during mouse vascular development. Bold arrows indicate new pathways identified by this study. See "Discussion" for details.

would rescue the *Ptch1* phenotype if it were caused by increased Dll4. At E8.5, PECAM1-stained *Ptch1*<sup>-/-</sup>; *Dll4*<sup>+/-</sup> embryos showed the same hollow, sinus-like structure and lack of a cranial plexus network observed in *Ptch1*<sup>-/-</sup> littermates (Figure 4D). These results show that reducing Dll4 levels in *Ptch1* mutants is not sufficient to rescue the *Ptch1* mutant vascular phenotype.

## Discussion

Hh signaling is a key regulator of vascular development, essential to the assignment of arterial identity to endothelial cells in zebrafish<sup>4</sup> and mice (this study), and the process of endothelial tubulogenesis.<sup>10</sup> Hh ligands are also known to induce expression of proangiogenic cytokines, including VEGF during neoangiogenesis in the adult<sup>11</sup> and during development of the coronary<sup>37</sup> and pulmonary<sup>13</sup> vascular systems. Interestingly, coronary vascular development appears to require both angiogenesis and vasculogenesis.<sup>38</sup> We have addressed whether during mouse vasculogenesis, Hh acts autonomously on endothelial cells, or indirectly via the proangiogenic cytokine VEGF to pattern blood vascular development and found Hh uses both VEGF-dependent and -independent mechanisms (Figure 5).

We found that Hh was required for the expression of VEGF specifically in those regions of the embryo in which Hh was necessary for artery/vein identity and endothelial tube formation. Notably, although Hh was necessary for VEGF expression, hyperactivation of the Hh pathway through deletion of *Ptch1* did not result in elevated VEGF levels. This result would suggest that during vasculogenesis, Hh may simply be required to derepress the VEGF locus, possibly by reducing levels of Gli repressors (the Gli isoform present in *Smo* mutants), whereas Gli activators (the Gli isoform present in *Ptch1* mutants) are not required for transcriptional activation of the VEGF locus, similar to how Hh regulates *Gremlin* expression during limb development.<sup>39-41</sup>

VEGF was sufficient in the absence of Hh signaling to promote Notch-dependent arterial identity and endothelial tube formation. These results confirm, we believe for the first time, that the Hh-VEGF-Notch signaling axis required for arterial specification during vasculogenesis in zebrafish is also active in mammalian development. Second, these results show that Hh is entirely dispensable for endothelial tube formation provided sufficient VEGF pathway activation occurs. The results presented here plus the report that endothelial specific deletion of *Smo* did not cause a vascular phenotype<sup>13</sup> strongly argue that Hh regulates endothelial tube formation and arterial identity during mouse vasculogenesis through regulation of VEGF expression rather than through an autonomous action on endothelial cells.

Our findings also demonstrate that Hh uses VEGF-independent means to pattern vessel development. *Ptch1* mutants displayed a vascular phenotype remarkably similar to that of the negative VEGF receptor *Flt1*,<sup>18</sup> including elevated expression of Dll4. Despite this, the *Ptch1* phenotype was not accompanied by dysregulated expression of VEGF or its major receptors. Forced activation of the Notch signaling pathway in endothelial cells (including by the overexpression of Dll4) results in an expansion of aortic vessel diameter at the expense of veins, and reduced branching morphogenesis.<sup>28,42</sup> Restoration of Dll4 to normal levels however, was not sufficient to overcome the *Ptch1* vascular phenotype, indicating the *Ptch1* phenotype was independent of Dll4 and Notch in general because Dll4 accounts for most if not all activation of Notch in the vasculature between E8.5 and E9.5.<sup>9,35,36</sup> Notably, mice engineered to overexpress Dll4 in endothelial cells (4-fold greater than normal) displayed a vascular phenotype that was less severe and occurred later than what we observed in *Ptch1* mutants, further arguing that the *Ptch1* phenotype could not be explained by dysregulated Dll4 expression.<sup>28</sup> Exactly why Dll4 is overexpressed in *Ptch1* mutants is unknown; however, we have excluded dysregulated VEGF signaling or misexpression of the VEGF-independent regulators of Dll4 transcription, *Foxc1* and *Foxc2*.

In addition to their tube formation defect, *Smo* dorsal aortas had aberrant connections to an ectopic vascular plexus under the lateral plate mesoderm. Although this arrangement is similar to veins, which have increased vascular density and connections compared with arteries,<sup>43</sup> it is unlikely this aspect of the *Smo* mutant phenotype occurs by the same mechanism that creates the difference between arteries and veins. Increased vascular density around veins is due to increased VEGF levels in venous territory,<sup>43</sup> whereas the increased vascular density around the dorsal aorta in *Smo* mutants occurs despite reduced VEGF expression. Instead we prefer a model in which an unidentified endothelial repellent normally expressed in the lateral plate mesoderm creates an avascular region adjacent to the dorsal aorta and this repellent is silenced in *Smo* mutant embryos. We do not believe the ectopic vessels in *Smo* mutants are responsible for the aorta tube formation defect (either because of diverted blood flow or because they are representative of failed aortic endothelial migration) for the following reasons: Ectopic vessel connections occurred in the posterior region of the *Smo* mutant embryo (where aorta formation was otherwise normal), failure of aorta tube formation in *VEGF*<sup>hypo</sup> mutant was not accompanied by ectopic vessel connections, and finally aorta tube formation was restored in *Smo*<sup>-/-</sup>; *Flt1*<sup>+/-</sup> embryos despite persistence of these ectopic vessels.

We summarize the effects of Hh on vascular development as follows (Figure 5): On the basis of the *Smo* mutant phenotype, Hh is required for endothelial tube formation through its regulation of VEGF, which we speculate is through regulation of lumen expansion (not initiation). In contrast sufficient activation of the Hh pathway, as occurs in *Ptch1* mutants, regulates tube diameter not by affecting lumen formation or expansion, but instead by reducing vascular density either through the fusion of many small vessel segments into one large vessel, or reduced endothelial sprouting or branching from a precursor vessel resulting in its increased size. *Ptch1* mutants underwent growth arrest before the onset of intersomitic vessel sprouting, the best characterized example of dorsal aorta branching morphogenesis, so we were unable to assess whether their dilated aorta diameter was caused by failed endothelial sprouting and migration such as occurs in Notch mutants<sup>28,42</sup> or another mechanism.

Because Ptc1 mutants undergo growth arrest before the onset of well-characterized examples of branching morphogenesis or plexus bed remodeling (key angiogenic events), we were unable to assess whether Ptc1 affects aspects of angiogenesis in the same way it affects vasculogenesis. In addition, whether the VEGF-independent Ptc1 phenotype acts autonomously, thereby directly affecting endothelial cell behavior, or nonautonomously via other proangiogenic factors known to be induced by Hh such as the angiopoietins,<sup>11</sup> remains to be established. These will be important questions to resolve because Hh signaling is required in general for angiogenesis, and the growth of certain tumors overexpressing Hh ligand was recently found to depend on activation of the Hh pathway in neighboring stroma by tumor-derived ligand.<sup>44</sup> Because this is likely to induce a proangiogenic response by the stroma<sup>45</sup> a more comprehensive understanding of which cell types respond to the Hh ligand and how they respond during a proangiogenic response may help in devising strategies to treat such tumors.

## Acknowledgments

We thank Rong Mo for expert technical assistance and all members of the Rossant and Hui laboratories for insightful discussions.

This work was supported by grants from the National Cancer Institute of Canada Terry Fox Foundation, Genome Canada, and

the Canadian Cancer Society. R.M.H. holds a Canada Research Chair in Imaging, J.R. is a Distinguished Investigator of the Canadian Institutes of Health Research, and L.C. is a C. J. Martin postdoctoral fellow of the National Health and Medical Research Council (Canberra, Australia).

## Authorship

Contribution: L.C., C.-C.H., and J.R. conceived and designed the experiments and wrote the manuscript; L.C., E.N., G.A.A., J.C., and R.M.H. performed all experiments; and A.N. provided reagents.

Conflict-of-interest disclosure: R.M.H. is named as an inventor and coapplicant with the Hospital for Sick Children on a patent application "Resolution Improvement in Emission Optical Projection Tomography," PCT/CA2007/001637. The remaining authors declare no competing financial interests.

The current affiliation for Dr Coultas is The Walter and Eliza Hall Institute of Medical Research, Parkville, Australia.

Correspondence: Leigh Coultas, PhD, The Walter and Eliza Hall Institute of Medical Research, 1G Royal Parade, Parkville, Vic, 3050, Australia; e-mail: lcoultas@wehi.edu.au; or Janet Rossant, PhD, The Hospital for Sick Children, 555 University Ave, Toronto, ON M5G 1X8 Canada; e-mail: janet.rossant@sickkids.ca.

## References

- Shalaby F, Rossant J, Yamaguchi TP, et al. Failure of blood-island formation and vasculogenesis in Flk-1-deficient mice. *Nature*. 1995;376(6535):62-66.
- Byrd N, Grabel L. Hedgehog signaling in murine vasculogenesis and angiogenesis. *Trends Cardiovasc Med*. 2004;14(8):308-313.
- Coultas L, Chawengsaksophak K, Rossant J. Endothelial cells and VEGF in vascular development. *Nature*. 2005;438(7070):937-945.
- Lawson ND, Vogel AM, Weinstein BM. Sonic hedgehog and vascular endothelial growth factor act upstream of the Notch pathway during arterial endothelial differentiation. *Dev Cell*. 2002;3(1):127-136.
- Gridley T. Notch signaling in vascular development and physiology. *Development*. 2007;134(15):2709-2718.
- Villa N, Walker L, Lindsell CE, Gasson J, Iruela-Arispe ML, Weinmaster G. Vascular expression of Notch pathway receptors and ligands is restricted to arterial vessels. *Mech Dev*. 2001;108(1-2):161-164.
- Del Amo FF, Smith DE, Swiatek PJ, et al. Expression pattern of Motch, a mouse homolog of *Drosophila* Notch, suggests an important role in early postimplantation mouse development. *Development*. 1992;115(3):737-744.
- Shirayoshi Y, Yuasa Y, Suzuki T, et al. Proto-oncogene of int-3, a mouse Notch homologue, is expressed in endothelial cells during early embryogenesis. *Genes Cells*. 1997;2(3):213-224.
- Duarte A, Hirashima M, Benedetto R, et al. Dose-sensitive requirement for mouse Dll4 in artery development. *Genes Dev*. 2004;18(20):2474-2478.
- Vokes SA, Yatskevich TA, Heimark RL, et al. Hedgehog signaling is essential for endothelial tube formation during vasculogenesis. *Development*. 2004;131(17):4371-4380.
- Pola R, Ling LE, Silver M, et al. The morphogen Sonic hedgehog is an indirect angiogenic agent upregulating two families of angiogenic growth factors. *Nat Med*. 2001;7(6):706-711.
- Kanda S, Mochizuki Y, Suematsu T, Miyata Y, Nomata K, Kanetake H. Sonic hedgehog induces capillary morphogenesis by endothelial cells through phosphoinositide 3-kinase. *J Biol Chem*. 2003;278(10):8244-8249.
- White AC, Lavine KJ, Ornitz DM. FGF9 and SHH regulate mesenchymal Vegfa expression and development of the pulmonary capillary network. *Development*. 2007;134(20):3743-3752.
- Damer A, Miquero L, Gertsenstein M, Risau W, Nagy A. Insufficient VEGFA activity in yolk sac endoderm compromises haematopoietic and endothelial differentiation. *Development*. 2002;129(8):1881-1892.
- Carmeliet P, Ferreira V, Breier G, et al. Abnormal blood vessel development and lethality in embryos lacking a single VEGF allele. *Nature*. 1996;380(6573):435-439.
- Long F, Zhang XM, Karp S, Yang Y, McMahon AP. Genetic manipulation of hedgehog signaling in the endochondral skeleton reveals a direct role in the regulation of chondrocyte proliferation. *Development*. 2001;128(24):5099-5108.
- Ellis T, Smyth I, Riley E, et al. Patched 1 conditional null allele in mice. *Genesis*. 2003;36(3):158-161.
- Fong GH, Rossant J, Gertsenstein M, Breitman ML. Role of the Flt-1 receptor tyrosine kinase in regulating the assembly of vascular endothelium. *Nature*. 1995;376(6535):66-70.
- Lickert H, Kutsch S, Kanzler B, Tamai Y, Taketo MM, Kemler R. Formation of multiple hearts in mice following deletion of beta-catenin in the embryonic endoderm. *Dev Cell*. 2002;3(2):171-181.
- Walls JR, Coultas L, Rossant J, Henkelman RM. Three-dimensional analysis of vascular development in the mouse embryo. *PLoS ONE*. 2008;3(8):e2853.
- Mukoyama YS, Gerber HP, Ferrara N, Gu C, Anderson DJ. Peripheral nerve-derived VEGF promotes arterial differentiation via neuropilin 1-mediated positive feedback. *Development*. 2005;132(5):941-952.
- Mukoyama YS, Shin D, Britsch S, Taniguchi M, Anderson DJ. Sensory nerves determine the pattern of arterial differentiation and blood vessel branching in the skin. *Cell*. 2002;109(6):693-705.
- Ferrara N, Carver-Moore K, Chen H, et al. Heterozygous embryonic lethality induced by targeted inactivation of the VEGF gene. *Nature*. 1996;380(6573):439-442.
- Miquero L, Langille BL, Nagy A. Embryonic development is disrupted by modest increases in vascular endothelial growth factor gene expression. *Development*. 2000;127(18):3941-3946.
- Kendall RL, Thomas KA. Inhibition of vascular endothelial cell growth factor activity by an endogenously encoded soluble receptor. *Proc Natl Acad Sci U S A*. 1993;90(22):10705-10709.
- Ferrara N, Gerber HP, LeCouter J. The biology of VEGF and its receptors. *Nat Med*. 2003;9(6):669-676.
- Rowitch DH, S-Jacques B, Lee SM, Flax JD, Snyder EY, McMahon AP. Sonic hedgehog regulates proliferation and inhibits differentiation of CNS precursor cells. *J Neurosci*. 1999;19(20):8954-8965.
- Trindade A, Kumar SR, Schemel JS, et al. Overexpression of delta-like 4 induces arterialization and attenuates vessel formation in developing mouse embryos. *Blood*. 2008;112(5):1720-1729.
- Taylor KL, Henderson AM, Hughes CC. Notch activation during endothelial cell network formation in vitro targets the basic HLH transcription factor HESR-1 and downregulates VEGFR-2/KDR expression. *Microvasc Res*. 2002;64(3):372-383.
- Williams CK, Li JL, Murga M, Harris AL, Tosato G. Up-regulation of the Notch ligand Delta-like 4 inhibits VEGF-induced endothelial cell function. *Blood*. 2006;107(3):931-939.
- Hayashi H, Kume T. Foxc transcription factors directly regulate Dll4 and Hey2 expression by interacting with the VEGF-Notch signaling pathways in endothelial cells. *PLoS ONE*. 2008;3(6):e2401.
- Abid MR, Shih SC, Otu HH, et al. A novel class of vascular endothelial growth factor-responsive genes that require forkhead activity for expression. *J Biol Chem*. 2006;281(46):35544-35553.

33. Minami T, Horiuchi K, Miura M, et al. Vascular endothelial growth factor- and thrombin-induced termination factor, Down syndrome critical region-1, attenuates endothelial cell proliferation and angiogenesis. *J Biol Chem.* 2004;279(48):50537-50554.
34. Seo S, Fujita H, Nakano A, Kang M, Duarte A, Kume T. The forkhead transcription factors, Foxc1 and Foxc2, are required for arterial specification and lymphatic sprouting during vascular development. *Dev Biol.* 2006;294(2):458-470.
35. Gale NW, Dominguez MG, Noguera I, et al. Haploinsufficiency of delta-like 4 ligand results in embryonic lethality due to major defects in arterial and vascular development. *Proc Natl Acad Sci U S A.* 2004;101(45):15949-15954.
36. Krebs LT, Shutter JR, Tanigaki K, Honjo T, Stark KL, Gridley T. Haploinsufficient lethality and formation of arteriovenous malformations in Notch pathway mutants. *Genes Dev.* 2004;18(20):2469-2473.
37. Lavine KJ, White AC, Park C, et al. Fibroblast growth factor signals regulate a wave of Hedgehog activation that is essential for coronary vascular development. *Genes Dev.* 2006;20(12):1651-1666.
38. Lavine KJ, Long F, Choi K, Smith C, Ornitz DM. Hedgehog signaling to distinct cell types differentially regulates coronary artery and vein development. *Development.* 2008;135(18):3161-3171.
39. te Welscher P, Zuniga A, Kuijper S, et al. Progression of vertebrate limb development through SHH-mediated counteraction of GLI3. *Science.* 2002;298(5594):827-830.
40. Litingtung Y, Dahn RD, Li Y, Fallon JF, Chiang C. Shh and Gli3 are dispensable for limb skeleton formation but regulate digit number and identity. *Nature.* 2002;418(6901):979-983.
41. Vokes SA, Ji H, Wong WH, McMahon AP. A genome-scale analysis of the cis-regulatory circuitry underlying sonic hedgehog-mediated patterning of the mammalian limb. *Genes Dev.* 2008;22(19):2651-2663.
42. Kim YH, Hu H, Guevara-Gallardo S, Lam MT, Fong SY, Wang RA. Artery and vein size is balanced by Notch and ephrin B2/EphB4 during angiogenesis. *Development.* 2008;135(22):3755-3764.
43. Claxton S, Fruttiger M. Role of arteries in oxygen induced vaso-obliteration. *Exp Eye Res.* 2003;77(3):305-311.
44. Yauch RL, Gould SE, Scales SJ, et al. A paracrine requirement for hedgehog signalling in cancer. *Nature.* 2008;455(7211):406-410.
45. Scales SJ, de Sauvage FJ. Mechanisms of Hedgehog pathway activation in cancer and implications for therapy. *Trends Pharmacol Sci.* 2009;30(6):303-312.